AQUA
Water Infrastructure, Ecosystems and Society

IWA PUBLISHING

 AQUA — Water Infrastructure, Ecosystems and Society Vol 71 No 10, 1148 doi: 10.2166/aqua.2022.076

Adsorption of brilliant green dye by used-tea-powder: equilibrium, kinetics and thermodynamics studies

Sarika Vithalkar[a,*], R. M. Jugade[a] and D. Saravanan[b]

[a] Department of Chemistry, R.T.M. Nagpur University, Nagpur 440033, India
[b] National College, Tiruchirapalli, Tamilnadu, India
*Corresponding author. E-mail: vithalkarsarika@gmail.com

ABSTRACT

The present research is based on the removal of Brilliant Green (BG) dye from its aqueous solution. Used-tea-powder (UTP) was used as a potential adsorbent to remove BG from aqueous solution. Pore morphology, surface properties, crystalline nature and thermal stability of UTP were assessed by using SEM, FTIR, XRD and TGA analysis. The optimized working conditions were found to be pH 6, UTP dose 100 mg, adsorption time 60 min and BG concentration 100 mg L^{-1}. The q_{max} obtained from the Langmuir model was 101.01 mg g^{-1} showing the utility of UTP in dye removal. The breakthrough volume and efficiency of the column were evaluated through column adsorption studies in fixed-bed mode. It was found that the pseudo-second-order kinetics model was followed as evaluated by the correlation studies. The calculated thermodynamic parameters showed that the adsorption process was feasible, exothermic and spontaneous.

Key words: adsorption, adsorption isotherms, adsorption kinetics, Brilliant Green, green adsorbent, used-tea-powder

HIGHLIGHTS

- Used-tea-powder (UTP) has been reported for the removal of Brilliant Green (BG) dye from water.
- The UTP is excellent adsorbent with capacity of 101.01 mg BG per gram of UTP.
- Fixed bed as well as column studies have been reported.
- Excellent eco-friendly biomaterial for water treatment.
- First ever report of UTP for BG dye removal.

GRAPHICAL ABSTRACT

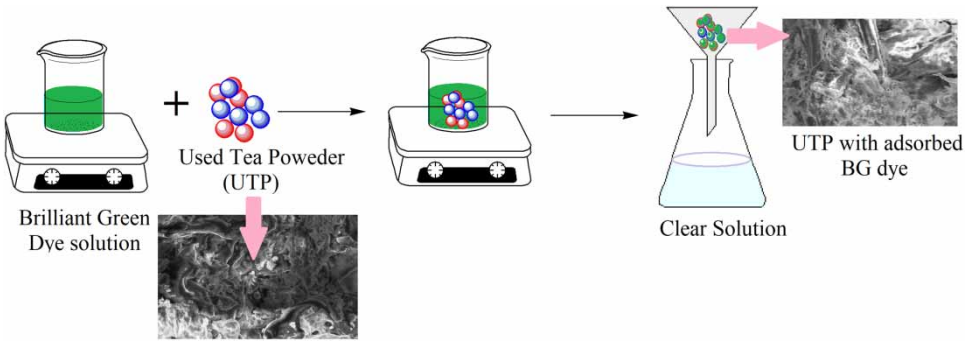

INTRODUCTION

In recent years, the introduction of dyes, coloring agents and pigments into the water bodies from a wide range of toxic derivatives, mainly from the dyestuff manufacturing and textile industries and also from food coloring, cosmetics, paper, paints, pulp, carpet and printing industries has increased considerably (Berradi *et al.* 2019; Slama *et al.* 2021). Due to the interest of consumers in stability and fastness, dye producers are producing chemically designed dyestuffs that are more difficult to

degrade by oxidizing agents, light and high temperatures after use. Unless properly treated, the dyes present in wastewater can reduce photosynthetic activity, which is due to interference of receiving streams with the transmission of sunlight and poses a serious hazard to most aquatic living organisms (Slama *et al.* 2021). Many dyes can cause skin diseases and have cancer-causing, mutagenetic impacts, etc. (Khan & Malik 2018). They are also responsible for esthetic pollution, eutrophication and distress in aquatic life (Khapre *et al.* 2021). The main reason for the release of hazardous substances in water is the oxidation and reduction of these dyes and hence demands the treatment of such coloring waste water before discharge into the water bodies (Mansoura *et al.* 2020).

On the basis of the structure of the dye molecules, dyes are classified as anionic (direct, acid and reactive dyes), nonionic (disperse and vat dyes) and cationic (base dyes) (Tan *et al.* 2015; Khapre and Jugade 2021). Among these, cationic dyes have the most dangerous and toxic effects as compared to anionic dyes in the atmosphere of receiving water and on the environment (Loqman *et al.* 2017). Brilliant green is an odorless cationic dye also known as diamond green G, solid green, ethyl green and basic green1 have various uses such as biological smudge, dermatological agent, veterinary medicine, an additive to poultry feed to restrain mold propagation, intestinal parasites, fungus, in textile dying, in manufacturing of inks for printing papers, etc.(Mansoura *et al.* 2020).

The methods used for the treatment of dye-contaminated effluents are chemical coagulation–flocculation, biological methods, oxidation processes, reverse osmosis, etc. (Qi *et al.* 2020). However, most of them involve a high operational cost when scaled-up to effluent treatment plant (ETP) scale. Adsorption processes using low-cost adsorbents are preferred over these methods (Pandey *et al.* 2022; Kaur *et al.* 2022; Saruchi Kumar *et al.* 2022). Depending upon the dye, the performance of low-cost adsorbents would vary. Biomasses and agricultural wastes such as rice husk, wheat bran, waste apricot, fly ash, peanut hull, coffee waste, peanut shell, etc. have been reported as potential adsorbents recently by various workers (Adegoke & Bello 2015).

Tea is the most common beverage in India, and so tea powder is used in every house. Used tea powder is another waste material that can be used as an adsorbent (Bansal *et al.* 2020). Recent literature shows the application of algal biomass for the removal of organic dyes from water bodies (Aragaw & Bogale .2021). Al-Maliki (2018) has shown that the chemical composition of algal biomass and tea waste is almost similar, including carbon, nitrogen, phosphorous, carbohydrates, as well as metal content. Considering these two aspects, it was hypothesized that the tea-waste produced in large amounts by Indian kitchens could be used for detoxification of dye-effluents.

Brilliant Green (BG) dye is a common dye used as a biological stain, dermatological agent, veterinary medicine, etc. It is known for its toxicity if it is exposed to skin or eyes, and also on ingestion. It might produce toxic gases like carbon dioxide, sulfur oxides and nitrogen oxides on decomposition that may be inhaled, causing lung toxicity (NO, NO_2) (Pandey *et al.* 2020; Nananwar *et al.* 2022). In the present study, the used-tea-powder (UTP) has been used as an excellent adsorbent for Brilliant Green (BG) dye in batch and column adsorption studies.

METHODS

Materials

Tea dust was purchased from a local manufacturer (Brook Bond Red Label, product code, F12B, India). Analytical grade sodium hydroxide (NaOH) (98%), hydrochloric acid (HCl) (35% aqueous solution, B. Pt. 110 °C) and Brilliant Green dye (dye content 95%) were procured from Loba Chemie, India. Double distilled water was used to prepare aqueous solutions. All of the reagents were analytical grade and did not need to be purified further.

Preparation of adsorbent

The tea powder is generally boiled in water, the aqueous extract is used for drinking purposes, while the solid residue is discarded, producing a solid waste. Hence, it was boiled multiple times to remove all the extractable contents and colors, while the residue was dried and used as an adsorbent. Tea dust was extracted with hot water multiple times until it stopped producing color. The extract was discarded and the solid residue was dried in a hot air oven at 50 °C for 24 h. The dried powder was sieved through a normal 500-micron sieve and was labeled as UTP. For future usage, the sorbent was stored in an airtight container.

Instruments

To determine the functional groups of UTP, a Bruker Alpha FT-IR spectrometer (USA), working between 500 and 4,000 cm^{-1} and averaging 23 scans for each recording, was used. The XRD pattern was recorded by an X'PERT-3 Powder X-ray

diffractometer (Malvern Panalytical Ltd, UK) using a 3kW X-ray source to investigate the crystalline structure of UTP. A scanning electron microscope (SEM) image was obtained by model Carl Zeiss EVO 18, Germany and the surface morphology of UTP was observed, with simultaneous evaluation of EDX using a hyphenated instrument. An EQ-824 spectrophotometer (Equiptronics, India, 350–900 nm) with matched quartz cuvettes (Shimadzu) was used for quantitation of BG in the solution. The Shimadzu DTG-60 working up to a temperature range of 1,000 °C under a nitrogen atmosphere at a heating rate of 20 °C min^{-1} was used for thermal stability studies on the basis of thermogravimetry and differential thermal analysis.

Batch adsorption studies

In order to optimize various operating parameters and to carry out equilibrium studies, a 25 mL BG solution of the desired concentration (25–400 mg L^{-1}) was taken in a stoppered conical flask. The pH of the solution was set using diluted HCl or NaOH solution from 4.0 to 9.0. It was added with the desired amount of UTP (10–150 mg) and shaken for the desired time (5–120 min) at 180 rpm. After the pre-decided contact time, the solution was filtered and the absorbance of the dye solution was determined spectrophotometrically at 625 nm. The percentage dye removal was calculated using Equation (1) below.

$$\% \, Removal = \frac{C_o - C_e}{C_o} \times 100 \tag{1}$$

where C_0 and C_e are the initial and equilibrium concentrations of BG.

RESULTS AND DISCUSSION

Characterization of UTP

As the UTP is not a single pure organic compound, its nature is complex with various functional groups, morphology and elemental composition. The FT-IR spectroscopy reveals a peak at 3,650 cm^{-1} (Figure 1(a)) indicating O-H group stretching. The aliphatic C–H group stretching might be ascribed to the bands detected at about 2,860 cm^{-1}. A shoulder may be seen at wave number 1,730 cm^{-1}, which could be attributable to the carbonyl stretch of carboxyl. The C-O stretching mode conjugated with the NH_2 is represented by the dip at 1,610 cm^{-1}. The 1,095 cm^{-1} band is an alcoholic group with a strong C-O-C stretching vibration. The findings are in line with those reported in the literature (Sikdar *et al.* 2020).

The XRD pattern is predicted to exhibit crystallinity. Figure 1(b) shows the XRD pattern of UTP and BG-adsorbed-UTP. It is obvious that the two XRD suggest the presence of crystalline regions. No notable change was observed in the XRD pattern after adsorption of BG. However, after dye adsorption, the reduction in peak heights of most of the peaks is an indication of a reduction in crystallinity (Bajpai & Jain 2012).

In a nitrogen atmosphere, thermogravimetric analysis (TGA) was used to investigate the material's thermal degradation profile. Figure 1(c) shows the UTP's thermogram. The sample shows three stages of weight loss. In the first stage, a mass loss of around 10% was observed around 100 °C due to moisture and trapped water evaporation. This was accompanied by endotherm on the DTA curve. When the cellulose and hemicellulose components began to break down, a second weight loss was observed between 200 and 400 °C. It was immediately followed by a third weight loss, leading to complete decomposition of the sample up to 600 °C due to lignin break down. Both of these decompositions were exothermic in nature, as shown by the DTA curve (Hu *et al.* 2001).

The EDS curve of UTP (Figure 1(d)) showed a considerable concentration of carbon along with calcium similar to activated carbon**.** SEM micrographs of UTP samples before and after dye adsorption (Figure 1(e) and 1(f)) revealed that the UTP possesses a rough surface morphology of fibers with significant porous and uneven surface structure. BG-loaded adsorbent showed uniform coverage of UTP by BG, leading to a reduction in surface porosity. This surface characteristic will substantiate the higher adsorption capacity.

Batch adsorption experiments

The pH point of zero charge (pHpzc) is a critical parameter that defines the linear range of pH sensitivity and, as a result, the kind of surface-active centers and the surface's adsorption ability (Khan *et al.* 2016). It was evaluated by stirring 100 mg of UTP with 25 mL of 0.1 M NaCl solutions having different initial pH values of 3.0–9.0. Stirring was continued for 24 h, followed by filtration of the solutions. The final pH of filtrates was recorded and a graph of pH change versus initial pH was plotted. The value of pHpzc is the point of x-intercept (Figure 2(a)). The value obtained from the graph was 6.2.

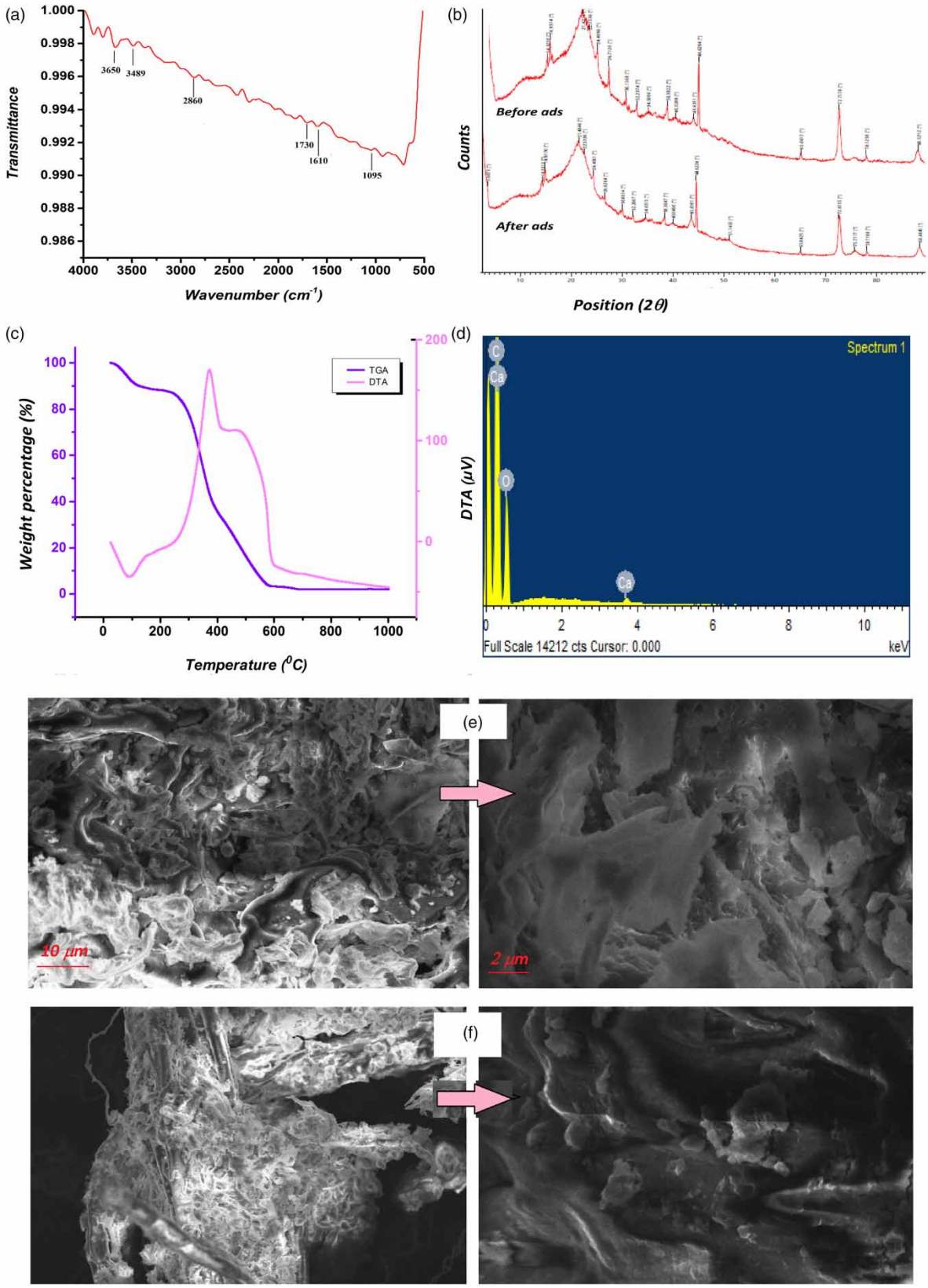

Figure 1 | (a) FTIR Spectra of UTP (b) XRD pattern of UTP and BG loaded UTP (c) TGA and DTA curves of UTP (d) EDX spectrum of UTP (e) SEM images of UDP at two different resolutions (f) SEM images of UDP with adsorbed BG at two different resolutions.

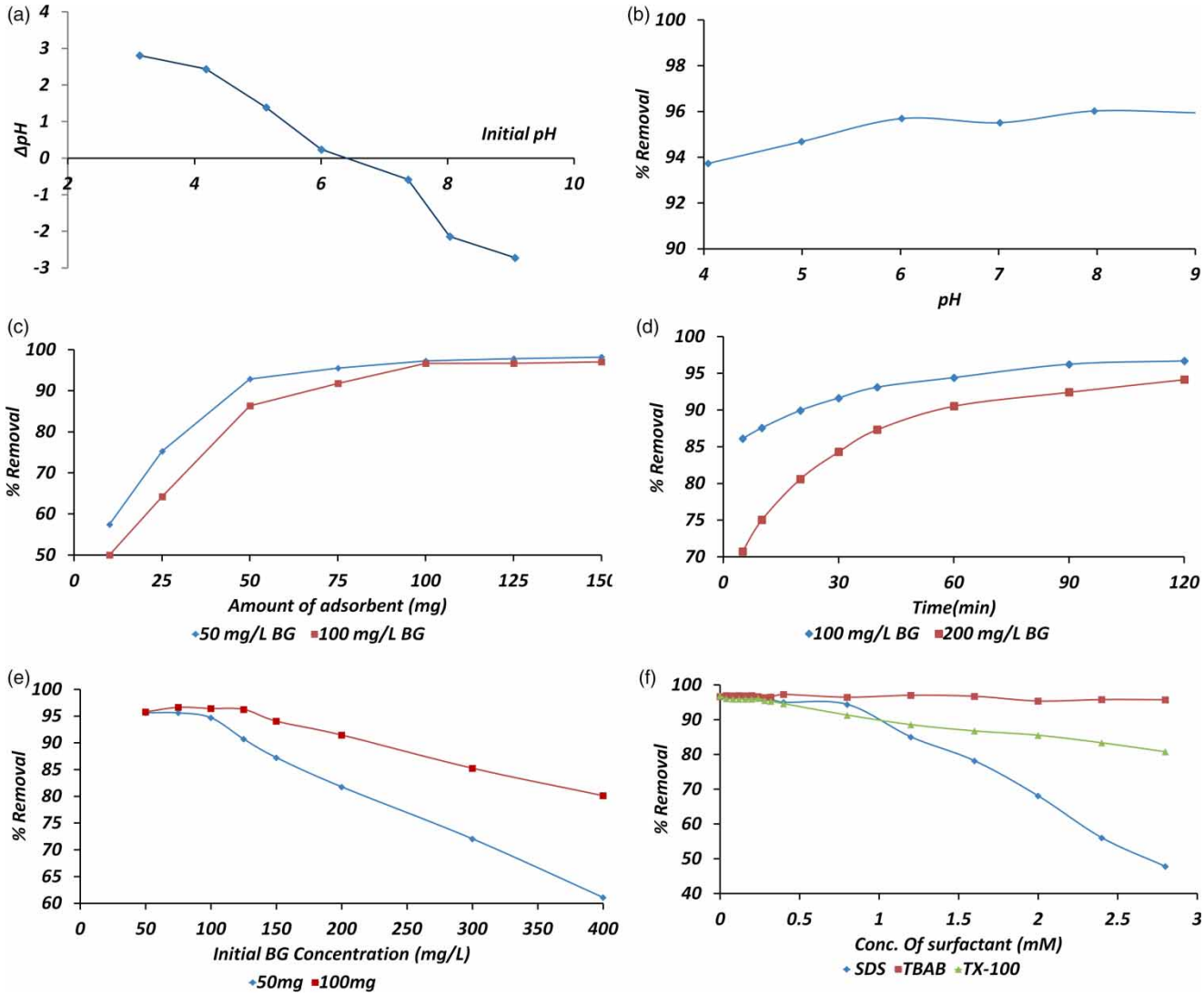

Figure 2 | Effect of (a) pHpzc, (b) pH (c) UTP dose, (d) adsorption time, (e) initial BG concentration (f) Effect of surfactants on percentage BG removal.

The influence of pH was examined using a dye concentration of 100 mg L^{-1}, UTP dose of 100 mg, a solution volume of 25 mL and a stirring time of 60 min. The initial pH values were adjusted from 4.0 to 9.0. The results reveal that over the whole pH range, there was no substantial change in the dye elimination. The percentage removal was between 94 and 96% over the entire pH range. This means that neither the H^+ nor the OH^- ions may affect dye adsorption on the adsorbent. As a result, the original pH of the dye solution, which was around 6.0, was used for the whole adsorption study (Figure 2(b)).

Increasing the amount of adsorbent from 10 to 150 mg resulted in a consistent increase in percentage removal (Figure 2(c)) for two BG concentrations of 50 and 100 mg L^{-1}. The increase in accessible surface area and the increase in the number of adsorption sites are the key reasons behind this. More binding sites are accessible for the adsorption of BG onto the UTP surface at larger adsorbent doses; however, after the optimal dosage of 100 mg, no significant change in the percentage removal was seen. As a result, 100 mg of adsorbent was used for all studies.

The kinetics studies were carried out for BG concentrations of 100 and 200 mg L^{-1}. It was observed that whereas adsorption was initially rapid, after 60 minutes, the extent of adsorption remained nearly constant (Figure 2(d)). This is due to the fact that a significant number of unoccupied surface sites were initially available for adsorption, but they gradually saturated with time. As a result, 60 minutes was chosen as the optimal time for further work.

The dye concentration was increased from 25 to 400 mg L^{-1}. At first, a high percentage of dye solution was removed (up to 125 mg L^{-1}), which further led to saturation as BG concentration increased (Figure 2(e)). This is because sorbent aggregation at high concentrations lowers the specific surface area available for dye adsorption. The adsorption impact was greatest at a concentration of 100 mg L^{-1}; hence, it was chosen for all investigations.

Most of the dye-containing effluents are also contaminated with surfactants. In order to study the effect of surfactant concentration on BG adsorption efficiency, three surfactants were selected. Anionic surfactant sodium dodecyl sulfate (SDS), cationic surfactant tetrabutyl ammonium bromide (TBAB) and nonionic surfactant Triton X-100 were added one by one to a 100 mg L^{-1} BG solution and adsorption efficiencies were recorded under optimized conditions. It can be observed from Figure 2(f) that TBAB has a negligible effect; Triton X-100 has a moderate effect, while SDS has a remarkable effect on the adsorption efficiency of UTP. This can be attributed to ionic interactions between anionic SDS and cationic dye molecules.

Adsorption isotherms

Adsorption isotherms describe the interactions between adsorbates and adsorbents. The extent of affinity between the sorbent surface and sorbate molecules, as well as the surface characteristics of the adsorbent, may be determined using an adsorption isotherm.

The Langmuir model assumes that adsorption occurs on a homogenous adsorbent surface, where all surface sites have equal attraction for adsorbate molecules and all positions are equivalent in terms of binding energies (Langmuir 1918). The linearized Langmuir isotherm can be represented as in Equation (2).

$$\frac{C_e}{q_e} = \frac{1}{q_m^b} + \frac{C_e}{q_m} \tag{2}$$

The Langmuir isotherm coefficients are q_m (mg g^{-1}) and b (L mg^{-1}).

The highest adsorption capacity is represented by q_m which was found out to be 101.01 mg g^{-1}. Figure 3(a) is a graphic representation of the model. The R^2 value was discovered to be 0.978.

The Freundlich isotherm espouses that the adsorbent surface is heterogeneous, and so the adsorbent sites are unequally distributed (Freundlich 1906). Its linearized equation can be expressed as Equation (3).

$$ln(q_e) = \frac{1}{n} lnC_e + lnK_f \tag{3}$$

K_f and n are Freundlich isothermal constants that represent adsorption capacity and adsorption intensity, respectively. The value of n was discovered to be 1.78, indicating favorable adsorption, while the value of R^2 was discovered to be 0.8362 (Figure 3(b)).

Table 1 shows the adsorption constants and correlation coefficients (R^2) for Langmuir and Freundlich isotherms. When the R^2 values were compared, the Langmuir model was the best-fit for the adsorption of BG dye solution on UTP surfaces, with a correlation coefficient near 1.0. This shows that a BG monolayer has formed on the UTP surface.

Kinetics of adsorption

The kinetic data acquired from batch studies of BG dye on to the UTP was examined for pseudo-first-order (PFO) and pseudo-second-order (PSO) models (Table 2). The studies were carried out using 25 mL of 100 mg L^{-1} of BG solutions, varying the contact time (5–120 min). The equation for pseudo-first-order kinetics is as follows: (Equation (4)) (Vithalkar & Jugade 2020).

$$log(q_e - q_t) = logq_e - \frac{k_1 t}{2.303} \tag{4}$$

where q_e and q_t are the concentrations of BG adsorbed at equilibrium and at time t, respectively, while k_1 (min^{-1}) denotes the first-order rate constant. With a regression coefficient of 0.9616, the plot of log(q_e-q_t) versus t was determined (Figure 3(c)).

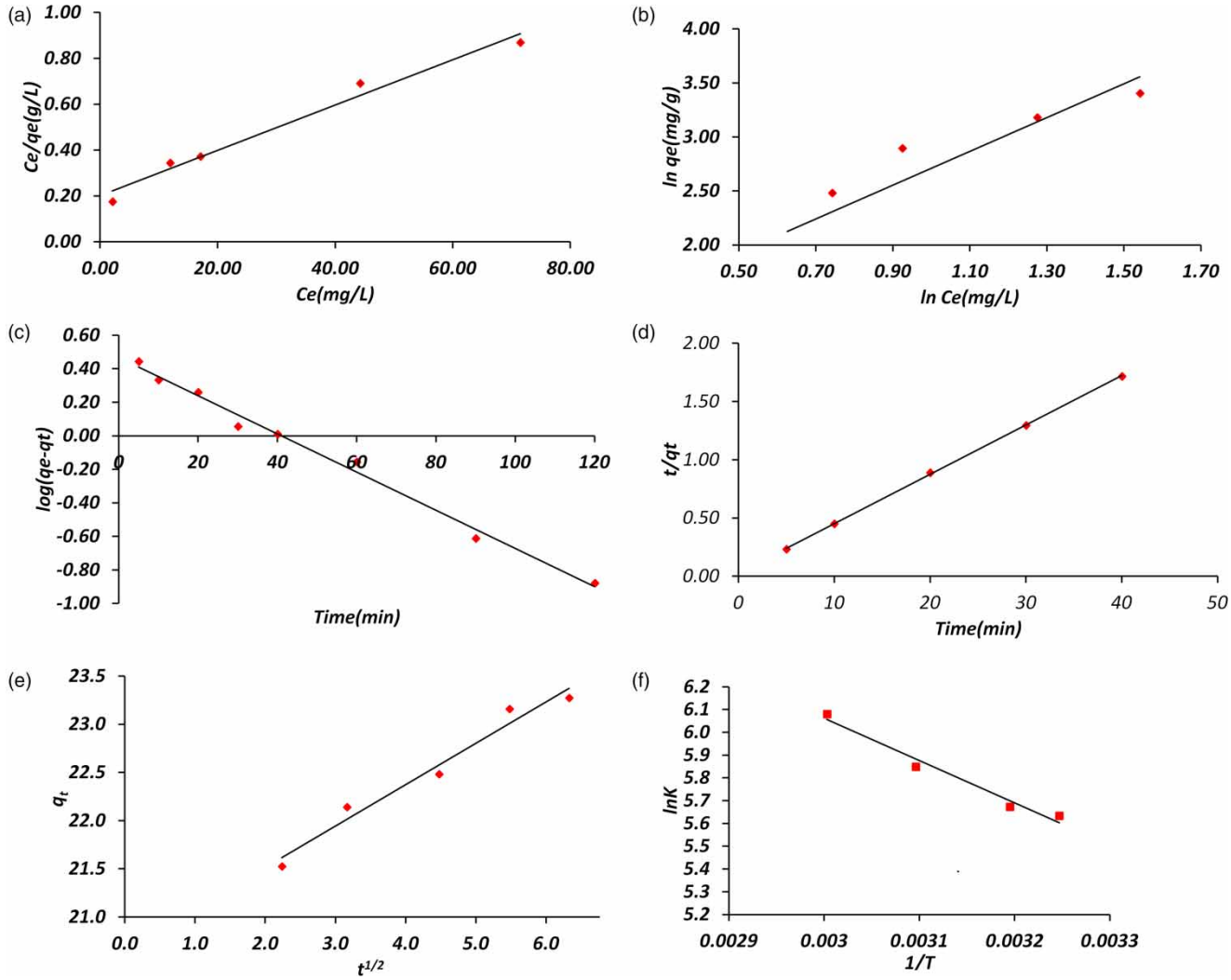

Figure 3 | (a) Langmuir adsorption isotherm (b) Freundlich adsorption isotherm, (c) Pseudo-first-order kinetics, (d) Pseudo-second-order kinetics (e) Intra-Particle Diffusion (f) Van't Hoff Plot.

Table 1 | Isotherm parameters

Langmuir			Freundlich		
q_m (mg g^{-1})	b (L g^{-1})	R^2	K_F (mg g^{-1})	n (g L^{-1})	R^2
101.01	5.714	0.978	8.49	1.78	0.8362

The pseudo-second-order rate equation is given by (Equation (5)) (Vithalkar & Jugade 2020).

$$\frac{t}{q_t} = \frac{1}{K_2 q_e^2} + \frac{t}{q_e} \tag{5}$$

The pseudo-second-order rate constant is k_2 (g mg^{-1} min^{-1}). The regression coefficient for log t/qt versus t is 0.9997, indicating a linear fluctuation (Figure 3(d)). The fact that the regression coefficient is near 1.0 indicates that the

Table 2 | Kinetics evaluation

PFO kinetics		PSO kinetics		Intraparticle diffusion	
$K_1(min^{-1})$	r^2	$k_2(g\ mg^{-1}\ min^{-1})$	r^2	$k_{int}(mg\ g^{-1}\ min^{1/2})$	r^2
0.023	0.9616	0.034	0.9997	0.34	0.958

pseudo-second-order kinetic model is the best match to describe the dye adsorption on the used-tea-powder. It is evident that the rate-determining phase in the adsorption phenomenon is chemisorption.

The Weber–Morris model can confirm whether intra-particle diffusion is the rate-determining phase during adsorption. q_t and $t^{1/2}$ of the adsorption process are related in this model as in Equation (6).

$$q_t = K_{int} \cdot t^{1/2} + C \tag{6}$$

Intraparticle diffusion is not the only rate-limiting step, as the plot of q_t vs $t^{1/2}$ does not pass through the origin. The slope represents the intraparticle rate constant k_{int} ($mg^{-1}\ g^{-1} min^{1/2}$) and the non-zero intercept indicates that diffusion is not the only rate-limiting phenomenon (Figure 3(e)).

Thermodynamics of adsorption

At 308 K, 313 K, 323 K and 333 K, the effect of temperature on BG adsorption at 200 mg L^{-1} was investigated in order to acquire relevant thermodynamic parameters. The adsorption free energy change (ΔG^o) is provided by Equation (7).

$$\Delta G^o = -RTlnK \tag{7}$$

The ratio of BG adsorbed on UTP to that in the solution phase was used to calculate the value of the equilibrium constant K. The Van't Hoff Equation (8) was used to calculate the values of entropy and enthalpy changes as:

$$ln\ K = (\Delta S^o/R) - (\Delta H^o/RT) \tag{8}$$

T is the absolute temperature (K), while R is the gas constant (8.314 J mol^{-1} K^{-1}). The slope and intercept of the plot of ln K versus 1/T were used to get the values of ΔH and ΔS. The thermodynamic parameters are shown in Table 3, and the Van't-Hoff plot is presented in Figure 3(f).

At all temperatures, Gibb's free energy change was negative, indicating that the adsorption process was spontaneous. The exothermic nature of the adsorption process is indicated by the negative enthalpy change, while the enhanced randomness at the solid-solution interface during the adsorption phase is indicated by the positive entropy change.

Flow through column parameters

Column investigations in fixed bed mode were also carried out to see if the adsorbent could be applied to a bigger sample. 500 mg of used tea powder was poured up to column heights of 5 cm in a glass column with a length of 20 cm and an internal diameter of 1.0 cm. A 50 mg L^{-1} BG solution was percolated through this column at a feed flow rate of 5 mL min^{-1}. The volume of eluate versus dye concentration plot yielded an S-shaped breakthrough curve (Figure 4). The plots were used to calculate various column parameters (Table 4). These findings demonstrate that greater sample volumes can be processed using column adsorption.

Table 3 | Thermodynamic parameters

ΔG (kJ mol^{-1})					
308 K	313 K	323 K	333 K	ΔH(kJ mol^{-1})	ΔS(J mol^{-1} K^{-1})
−45.264	−45.747	−46.715	−47.683	−15.458	96.77

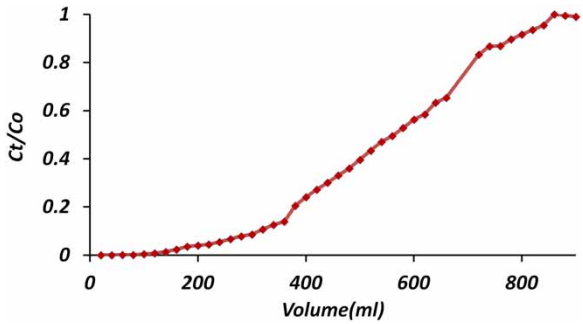

Figure 4 | Column studies.

Table 4 | Column parameters

Parameter	Result
Inlet dye concentration	50 mg L^{-1}
Breakthrough volume	320 mL
Exhaustion volume	800 mL
Breakthrough capacity	32 mg g^{-1}
Exhaustion capacity	80 mg g^{-1}
Degree of column utilization	40%

Table 5 | Comparison of adsorption capacities of various adsorbents towards brilliant green

S. N.	Adsorbent	Adsorption capacity (mg g^{-1})	Reference
1	Chemically activated guava seeds carbon	80.45	Mansoura *et al.* (2020)
2	Nano hydroxypatite/Chitosan composite	49.1	Ragab *et al.* (2019)
3	Pinus roxburghii leaves	71.42	Rehman *et al.* (2019)
4	Palm fronds activated carbon	45.45	Ahmad & Elchaghaby (2018)
5	NaOH treated saw dust	58.4795	Mane & Vijay (2011)
6	Crosslinked chitosan graft copolymers	17.6678	Özkahraman *et al.* (2011)
7	Kaolin	65.42	Nandi *et al.* (2009)
8	UTP	101.01	Present study

CONCLUSION

The current study shows that UTP can be employed as an efficient adsorbent for removing BG from aqueous solutions. pH 6.0, adsorbent dose 100 mg, contact period 60 min and dye concentration 100 mg L^{-1} were shown to be the best working conditions for the various parameters investigated. The high regression coefficient indicates that the pseudo-second-order kinetic model was used, with the Langmuir adsorption isotherm being the best fit. The thermodynamic parameters revealed that the process is spontaneous and exothermic, while positive entropy change indicates the enhanced randomness at the solid-solution interface during the adsorption phase. As indicated in Table 5, the adsorption capacity of BG onto UTP was determined to be 101.01 mg g^{-1}, which is significantly greater than most previously reported materials.

ACKNOWLEDGEMENT

Authors are thankful to DST, New Delhi for DST-FIST grant and UGC for UGC-SAP grant.

DATA AVAILABILITY STATEMENT

All relevant data are included in the paper or its Supplementary Information.

CONFLICT OF INTEREST

The authors declare there is no conflict.

REFERENCES

Adegoke, K. A. & Bello, O. S. 2015 Dye sequestration using agricultural wastes as adsorbents. *Water Resour. Ind.* **12**, 8–24.

Ahmad, A. F. & Elchaghaby, G. A. 2018 Palm fronds activated carbon for the removal of brilliant green dye from wastewater. *Water Desal. Res. J.* **2**, 1–10.

Al-Maliki, S. 2018 Interactions between mycorrhizal fungi, tea wastes and algal biomass affecting microbial community, soil structure and alleviating of salinity stress on corn yield (Zea mays L). *Plants* **7**, 63.

Aragaw, T. A. & Bogale, F. M. 2021 Biomass-based adsorbents for removal of dyes from wastewater: a review. *Front. Environ. Sci.* **9**, 764958.

Bajpai, S. & Jain, A. 2012 Equilibrium and thermodynamic studies for adsorption of crystal violet onto spent tea leaves (STL). *Water* **5**, 52–71.

Bansal, M., Patnala, P. K. & Dugmore, T. 2020 Adsorption of Eriochrome Black-T(EBT) using tea waste as a low cost adsorbent by batch studies: a green approach for dye effluent treatments. *CRGSC* **3**, 100036.

Berradi, M., Hsissou, R., Khudhair, M., Assouag, M., Cherkaoui, O., Bachiri, A. & Harfi, A. 2019 Textile finishing dyes and their impact on aquatic environs. *Heliyon* **5**, e02711.

Freundlich, H. M. 1906 Over the adsorption in solution. *J. Phys. Chem.* **57**, 385–471.

Hu, Z., Srinivasan, M. P. & Ni, Y. 2001 Novel activation process for preparing highly microporous and mesoporous activated carbons. *Carbon* **39** (6), 877–886.

Kaur, S. M., Kumar, V., Ghfar, A. A. & Pandey, S. A. 2022 Green approach for the synthesis of silver nanoparticle-Embedded chitosan bionanocomposite as a potential device for the sustained release of the itraconazole drug and its antibacterial characteristics. *Polymers* **14**, 1911.

Khan, S. & Malik, A. 2018 Toxicity evaluation of textile effluents and role of native soil bacterium in biodegradation of a textile dye. *Environ. Sci. Pollut. Res.* **25**, 4446–4458.

Khan, M. R., Rahman, W., Ong, H. R., Ismail, A. B. & Cheng, C. K. 2016 Tea dust as a potential low-cost adsorbent for the removal of crystal violet from aqueous solution. *Desalin. Water Treat.* **57**, 31.

Khapre, M. & Jugade, R. 2021 Tetrabutylammonium impregnated chitosan for adsorptive removal of harmful carcinogenic dyes from water-bodies. *Chemistry Africa* **4**, 993–1005.

Khapre, M., Saravanan, D., Pandey, S. & Jugade, R. 2021 Glutaraldehyde-cross-linked chitosan–alginate composite for organic dyes removal from aqueous solutions. *Int. J. Biol. Macromol* **190**, 862–875.

Langmuir, I. 1918 The adsorption of gases on plane surfaces of glass, mica and platinum. *J. Am.Chem. Soc.* **40**, 1361–1403.

Loqman, A., Bali, B., Lützenkirchen, J., Weidler, P. G. & Kherbeche, A. 2017 Adsorptive removal of crystal violet dye by a local clay and process optimization by response surface methodology. *Appl Water Sci.* **7**, 3649–3660.

Mane, V. S. & Vijay, P. V. 2011 Studies on the adsorption of Brilliant Green dye from aqueous solution onto low-cost NaOH treated saw dust. *Desalination* **273**, 321–329.

Mansoura, R., Simedab, G. & Zaatout, A. 2020 Adsorption studies on brilliant green dye in aqueous solutions using activated carbon derived from guava seeds by chemical activation with phosphoric acid. *Desalin. Water Treat.* **202**, 396–409.

Nananwar, P., Bakshe, P., Saravanan, D. & Jugade, R. 2022 Chitosan entrapped microporous activated carbon composite as a supersorbent for remazol brilliant blue R. *Materials Advances* **3**, 5488–5496.

Nandi, B. K., Goswami, A. & Purkait, M. K. 2009 Adsorption characteristics of brilliant green dye on kaolin. *J. Hazard. Mater.* **161**, 387–395.

Özkahraman, B., Bal, A., Acar, I. & Güçlü, J. 2011 Adsorption of brilliant green from aqueous solutions onto crosslinked chitosan graft copolymers. *Clean – Soil, Air, Water* **39** (11), 1001–1006.

Pandey, S., Do, J. Y., Kim, J. & Kang, M. 2020 Fast and highly efficient removal of dye from aqueous solution using natural locust bean gum based hydrogels as adsorbent. *Int. J. Biol. Macromol.* **143**, 60–75.

Pandey, S., Son, N. & Kang, M. 2022 Synergistic sorption performance of karaya gum crosslink poly(acrylamide-co-acrylonitrile) @ metal nanoparticle for organic pollutants. *Int. J. Biol. Macromol.* **210**, 300–314.

Qi, C., Chen, H., Xu, C., Xu, Z., Chen, H., Yang, S., Li, S., He, H. & Sun, C. 2020 Synthesis and application of magnetic materials-barium ferrite nanomaterial as an effective microwave catalyst for degradation of brilliant green. *Chemosphere* **260**, 127681.

Ragab, A., Ahmed, I. & Bader, D. 2019 The removal of brilliant green dye from aqueous solution using nano hydroxyapatite/chitosan composite as a sorbent. *Molecule* **24** (5), 847.

Rehman, R., Muhammad, S. & Arshad, M. 2019 Brilliant green and acid orange 74 dyes removal from water by Pinus roxburghii leaves in naturally benign way: an application of green chemistry. *J. Chem.* **2019**, 10.

Saruchi Kumar, V., Ghfar, A. A. & Pandey, S. 2022 Microwave synthesize karaya Gum-Cu, Ni nanoparticles based bionanocomposite as an adsorbent for malachite green dye: kinetics and thermodynamics. *Front. Mater.* **9**, 827314.

Sikdar, D., Goswami, S. & Das, P. 2020 Activated carbonaceous materials from tea waste and its removal capacity of indigo carmine present in solution: synthesis, batch and optimization study. *Sustain. Environ. Res.* **30**, 30.

Slama, H. B., Bouket, A., Pourhassan, Z., Alenezi, F. N., Silini, A., Cherif-Silini, H., Oszako, T., Luptakova, L., Golińska, P. & Belbahri, L. 2021 Diversity of synthetic dyes from textile industries, discharge impacts and treatment methods. *Appl. Sci.* **11**, 6255.

Tan, K. B., Vakili, M., Horri, B. A., Poh, P. E., Abdullah, A. Z. & Salamatinia, B. 2015 Adsorption of dyes by nanomaterials: recent developments and adsorption mechanisms. *Sep. Purif. Technol.* **150**, 229–242.

Vithalkar, S. H. & Jugade, R. M. 2020 Adsorptive removal of crystal violet from aqueous solution by cross-linked chitosan coated bentonite. *Mater. Today* **29** (4), 1025–1032.

First received 23 May 2022; accepted in revised form 9 September 2022. Available online 21 September 2022